International Journal of Engineering

Journal Homepage: www.ije.ir

High Temperature Corrosion Behavior of High Velocity Oxy Fuel Sprayed NiCrMoFeCoAl-30%SiO_2 and NiCrMoFeCoAl-30%Cr_2O_3 Composite Coatings on ASTM SA213-T22 Steel in a Coal-fired Boiler Environment

V. G. Patil*[a], B. Somasundaram[a], S. Kandaiah[b], S. kumar[a]

[a] *School of Mechanical Engineering, REVA University Bengaluru, India*
[b] *Department of Chemistry, School of Applied Sciences, REVA University Bengaluru, India*

PAPER INFO

Paper history:
Received 06 February 2022
Received in revised form 23 April 2022
Accepted 24 April 2022

Keywords:
Hot Corrosion
High-velocity Oxy Fuel
Thermogravimetric Analysis
Thermal Spraying
Oxide Scale

ABSTRACT

High-velocity oxy fuel (HVOF) sprayed coatings can improve the corrosion resistance of bare ASTM SA213-T22 boiler steel. In this report, we have investigated the NiCrMoFeCoAl-30%SiO_2 and NiCrMoFeCoAl-30%Cr_2O_3 composite coatings were deposited on bare ASTM SA213-T22 boiler steel for corrosion protection. High-temperature corrosion studies were conducted in a molten salt (Na_2SO_4-60%V_2O_5) environment at 700ºC under thermo-cyclic conditions. The as-sprayed composite coatings are characterized for microstructure and mechanical properties. The thermo-gravimetric method was utilized to understand the kinetics of corrosion. Characterization of the corrosion products was examined by using scanning electron microscope (SEM)/ Energy dispersive spectroscopy (EDS) and X-ray diffraction (XRD) techniques. The obtained results suggest both the composite coatings are favorable to corrosion resistance over the bare ASTM SA213-T22 boiler steel. The NiCrMoFeCoAl-30%Cr_2O_3 composite coating was concluded to present a superior corrosion resistance in the high-temperature corrosion environment because of the uniform distribution of the composite coating matrix and the development of protective protection Cr_2O_3 in the scale. The molten salt heat-treated chromium oxide containing coating shows good corrosion stability than the silica composite. This could be attributed to the high temperature assisted formation metal chromates, chromites and oxide layers.

***doi**: 10.5829/ije.2022.35.07a.19*

1. INTRODUCTION

High-performance coatings formulated on the surface of materials by thermal spraying technology are among the most efficient methods to enhance corrosion, wear, and oxidation resistance properties and extend their lifespan [1-5]. Generally, the boiler steel materials were subjected to high-temperature environment and corrosive conditions in industries. Several coating methods were used to protect the boiler steel alloy [1-5]. Singh et al. [6] had investigated the performance of uncoated T-91 steel and HVOF coated Ni-20Cr & (Cr_3C_2–25 (Ni–20Cr) steels which were subjected to 40%Na_2SO_4–V_2O_5 environment at 900°C. The Cr_3C_2–25(Ni–20Cr) coated steel was superior towards corrosion resistant than the Ni-20Cr coated steel. The uncoated T-91 steel was found to gain higher weight. AK et al. [7] reported that the HVOF method can be used to fabricate better carbide-metal coating along with good bond strength, high density, low decarburization, and high hardness. Sidhu et al. [8] had examined the behavior of bare and HVOF coated samples after high-temperature treatment in Na_2SO_4–60%V_2O_5 environment at 900°C. The NiCr coated steel was ascertained to be very effective for corrosion resistance than the bare steel. The bare sample shows the spalling of oxide scales during high-temperature corrosion. Thermal spray technology is a rapidly developing surface engineering area and is

*Corresponding Author Email: patilviresh751@gmail.com (V. G. Patil)

Please cite this article as: V. G. Patil, B. Somasundaram, S. Kandaiah, S. kumar, High Temperature Corrosion Behavior of High Velocity Oxy Fuel Sprayed NiCrMoFeCoAl-30%SiO_2 and NiCrMoFeCoAl-30%Cr_2O_3 Composite Coatings on ASTM SA213-T22 Steel in a Coal-fired Boiler Environment, ***International Journal of Engineering, Transactions A: Basics***, Vol. 35, No. 07, (2022) 1416-1427

extensively employed to protect metallic surfaces against high-temperature corrosion [9, 10]. The HVOF coated samples are advantageous to corrosion resistance. Degradation occurs especially within the hot sections of boilers due to hot corrosion [11]. Goyal et al. [12] had studied the performance of uncoated and HVOF coated T22 specimens were subjected to the molten salt environment at 700°C. The results exposed that bare ASTM-SA213- T22 steel suffered spallation of the Fe_2O_3 scale. The HVOF coated T22 steel specimens showed lower weight gain with corrosion resistance. Mahesh et al. [13] examined the high-temperature corrosion behavior of uncoated Superfer 800 and HVOF coated samples in an actual coal-fired boiler environment at 700°C for 1000 h. NiCrAl coated Superfer 800 sample exhibits superior corrosion resistance to hot corrosion than Ni–5Al coated Superfer 800 sample in an actual coal-fired boiler environment. Wang et al. [14] remarked in their research studies on the oil-fired power generators that the formulation of sulfate salts and ashes are the distinctive high-temperature corrosion origins. Sidhu et al. [15] had investigated the high-temperature corrosion behavior of uncoated (ASME SA213-T22 and T91) and HVOF coated 93WC-Cr_3C_2-7Ni, WC-17Co specimens which were exposed to an actual coal-fired boiler environment. The high-temperature corrosion resistance of 93(WC-Cr_3C_2)-7Ni-coated steel sample was better among all coated samples. Sreenivasulu and Manikandan [16] had studied the high-temperature corrosion behavior of uncoated alloy 80A, HVOF coated Cr3C2-25NiCr, and NiCrMoNb samples were subjected to the molten salt environment at 900°C. The Cr_3C_2-25NiCr coating had shown good corrosion resistance compared to bare alloy 80A. Chatha et al. [17] studied the hot corrosion behavior of uncoated and coated steels subjected to the molten salt environment at 750°C. The T91 boiler tube steel shows superior mass gain, because of the development of oxide scales (Fe_2O_3). The 80Ni–Cr coating was noticed to be very effective in corrosion resistance than the Cr_3C_2–25(Ni–20Cr) coating. The high-temperature corrosion reduces the corrosion-resistant properties of the boiler tube steels, conclusively resulting in the premature breakdown of boiler parts [18, 19]. Somasundaram et al. [20] were investigated the hot corrosion behavior of HVOF sprayed (60%Cr_3C_2–NiCr) +5 % Si coatings on Superfer 800 H, SA213-T22, and MDN-310 substrate alloys. The coated and uncoated samples were exposed to a molten salt environment at 700°C. It was observed that the HVOF coated samples presented more beneficial corrosion resistance than the bare samples. Mangla et al. [21] had explored the high-temperature corrosion behavior of HVOF and Plasma sprayed 80%Ni20%Cr coated SA-213-T22 steel exposed to the molten salt environment at 900°C. It concludes that HVOF sprayed coating exhibits a superior corrosion resistance than the PS method. Kaur et al. [22] were studied the behavior of uncoated T22 boiler steel and HVOF sprayed 75%Cr_3C_2-25%NiCr coated samples were subjected to the molten salt, air, and actual boiler environments for 50 cycles. The HVOF coated steel was noticed to be complete and spallation-free, while the uncoated T22 boiler steel was endured. Kaur et al. [22] explored the hot corrosion behavior of T22 bare steel utilized in boilers. The contaminations present in fuel employed such as Na, S, and V cause material corrosion. Reactions between these impurities in the presence of oxygen lead to ash deposits, like $NaVO_3$, Na_2SO_4, and V_2O_5, which cause harsh corrosion [23, 24]. Kaushal et al. [25] had explored the high-temperature corrosion performance of uncoated ASTM A213 347H boiler steel and HVOF coated Ni-20Cr samples in a Na_2SO_4-60%V_2O_5 environment at 900°C. The bare T22 steel endured a higher rate of deprivation and wide spallation. The 80Ni-Cr coating was effective in less weight gain and corrosion resistance. The coating enhances the lifespan of structural parts by protecting the surface against wear and corrosion [26-28]. Zhang et al. [29] were studied the high-temperature corrosion conflict of HVOF sprayed CoCrAlSiY coated steel with different Si (0wt%, 2wt%, and 5wt %) concentrations are exposed to 75% Na_2SO_4-25% NaCl at 900 ° C. An increase in Si concentration reduces the average corrosion diffusion depth of the HVOF coating. Thus, it helps to improve the corrosion resistance of the HVOF coating in the given environment. Saricimen et al. [30] were studied the high-temperature corrosion performance of HVOF and plasma sprayed Ni & Co-based metallic coated 310 stainless steel specimens are exposed to NaCl, Na_2SO_4, and V_2O_5 salt mixtures at 900°C. Experimental results indicate that Cobalt-based coatings perform better than Nickel-based coating. Sidhu et al. [31] were explored the high-temperature corrosion behavior of bare ASTM SA213-T11 steel and HVOF coated specimens are subjected to a Na_2SO_4-60%V_2O_5 environment at 900ºC. NiCr Coating presented a better corrosive resistance than uncoated steel and WC-Co & Cr_3C_2-NiCr coatings. Shi et al. [32] were investigated the high-temperature corrosion behavior of HVOF Cr_3C_2-NiCr/NiCrAlY coated UMCo50 alloy samples are subjected to the Na_2SO_4 environment at different temperatures. The results explored that the Cr_3C_2-NiCr coating was relatively dense and mainly compiled of Cr_3C_2, NiCr, and a minor quantity of Cr_7C_3 three phases. Table 1 illustrates the summary of the literature review.

In the current study, the composite coatings were formulated on ASTM SA213-T22 steel by using the HVOF technique. To the best of our knowledge, there is no reported literature on high-temperature corrosion behavior of HVOF sprayed NiCrMoFeCoAl-30%SiO_2 and NiCrMoFeCoAl-30%Cr_2O_3 composite coatings.

The degradation of T22 boiler steel is progressive when subjected to high-temperature industrial conditions.

TABLE 1. Summary of the literature review

S. No.	Year	Authors	Coating material	Substrate	Process	Remarks
1	2022	Ebrahimi et al. [1]	Bi-layered Hydroxyapatite /Al_2O_3-SiO_2 (with 10, 20, 30 %wt SiO_2) were deposited on Ti	Commercial pure Ti (ASTM grade #2)	Plasma spray	The composition of Al_2O_3-20% wt SiO_2 shows excellent protection which is attributed to their particular compositions, properties and microstructures.
2	2021	Spandana et al. [2]	YSZ/TiO_2 over NiCr bond coat	TV1 alloy of aluminium	Plasma spray HVOF	TBC coated piston shows the increase in brake thermal efficiency and decrease in brake specific fuel consumption compared to the uncoated piston.
3	2017	Rahnavard [3]	CYSZ/NiCrAlY	Inconel 738	Plasma spray	Functional grade material with thermal barrier - Very promising potential as a novel TBC material.
4	2013	Mhdipoor and Rahimipour [4]	Yttria stabilized zirconia (YSZ) and ceria stabilized zirconia (ZrO_2 $25CeO_2$ $2.5Y_2O_3$)	Ni-Based superalloy (Inconel738) and 1020 steel	Plasma spray	CSZ TBCs had better resistant to high temperature corrosion than YSZ TBCs.
5	2017	Naeimi and Tahari [5]	MCrAlY/ CoNiCrAlY	Inconel 738 Superalloy	HVOF	The increase of surface roughness as a result of the other oxides including Cr_2O_3, NiO, and spinel, inhomogeneous and non-uniform thermal oxide layer created and oxidation was constantly increased.
6	2016	Singh et al. [6]	Ni-20Cr & (Cr_3C_2–25 (Ni–20Cr)	T-91 steel	HVOF	The Cr_3C_2–25(Ni–20Cr) coated steel was good corrosion resistant to the Ni-20Cr coated steel.
7	2003	AK et al. [7]	80Ni-20Cr	Stainless steel	HVOF	HVOF with carbide-metal coating, exhibit good bond strength, low decarburization, high density and high hardness.
8	2006	Sidhu et al. [8]	Ni–20Cr	ASTM-SA-210 GrA1, ASTM-SA213 (T-11) and ASTM-SA213 (T-22)	HVOF	NiCr coated steel was ascertained to be good corrosion resistance than the substrate steel.
9	2003	Uusitalo et al. [9]	Ni50Cr Ni57Cr Ni21Cr9Mo	Ferritic steel Austenitic steel	HVOF	Ni-based coatings was good corrosion resistance than the ferritic steel.
10	1992	Wang et al. [10]	Chromized-siliconized	1018 carbon steel and 2.25 Cr-[Mo steel	Plasma spray	The chromized-siliconized coatings had lower material wastage in both the static and the dynamic oxidation tests than did the chromized-aluminized and straight chromized coatings
11	2002	Rapp [11]	-	-	-	An evolution of a negative solubility gradient as a criterion for continuing hot corrosion is made
12	2019	Goyal et al. [12]	Cr_2O_3–1wt%CNT Cr_2O_3–2wt%CNT Cr_2O_3–4wt%CNT Cr_2O_3–6wt%CNT Cr_2O_3–8wt%CNT	ASTM-SA213-T22 steel	HVOF	The T22 substrate steel suffered spallation of the Fe_2O_3 scale. The HVOF coated T22 substrate steel samples showed lower weight gains with corrosion resistance.
13	2010	Mahesh et al. [13]	NiCrAl and Ni–5Al	Superfer 800	HVOF	NiCrAl coated Superfer 800 sample exhibits good corrosion resistance to hot corrosion than Ni–5Al coated Superfer 800 sample in an actual coal-fired boiler environment.

14	2002	Wang et al. [14]	Na_2SO_4 coating	The tungsten-bearing and Al2O3-forming superalloy, MARM247,	-	The oil-fired power generators show that the formulation of sulfate salts and ashes are the distinctive hot corrosion origins.
15	2019	Sidhu et al. [15]	93WC-Cr_3C_2-7Ni WC-17Co	ASME SA213-T22 and T91	HVOF	The high-temperature corrosion resistance of 93(WC-Cr_3C_2)-7Ni-coated steel sample was better among all coated samples.
16	2018	Manikandan [16]	Cr_3C_2-25NiCr and NiCrMoNb	Alloy 80A	HVOF	The Cr_3C_2-25NiCr coating had shown good corrosion resistance as equated to substrate alloy 80A.
17	2012	Chatha et al. [17]	80Ni–Cr and Cr_3C_2–25(Ni–20Cr)	T91 boiler tube steel	HVOF	The 80Ni–Cr coating was noticed to be very effective in corrosion resistance than the Cr_3C_2–25(Ni–20Cr) coating.
18	2016	Loghman-Estarki et al. [18]	YSZ, ScYSZ, NiCrAlY	Ni-based supperalloy	Plasma spray	ScYSZ coating has more hot corrosion resistance than YSZ coatings
19	2018	Aadhavan et al. [19]	Ceria coating	AISI 304, AISI 410, Inconel 600	electron beam physical vapor deposition	The high-temperature corrosion reduces the properties of the boiler tube steels, conclusively resulting in the premature breakdown of boiler parts
20	2015	Somasundaram et al. [20]	(60%Cr_3C_2–NiCr) + 5 % Si	Superfer 800 H, SA213-T22, and MDN-310	HVOF	HVOF coated specimens displays more beneficial corrosion resistance than the bare samples.
21	2017	Mangla et al. [21]	80%Ni20%Cr	SA-213-T22	HVOF and Plasma spray	HVOF sprayed coating shows superior corrosion resistance than the PS method
22	2012	Kaur et al. [22]	75%Cr_3C_2-25%NiCr	SA-213-T22	HVOF	The HVOF coated steel was remarked to be complete and spallation-free, while the uncoated T22 boiler steel was endured.
23	2007	Sidhu et al. [23]	SiO_2 (60.27%), Al_2O_3 (25.46%), Fe_2O_3(6.02%), CaO (3.68%), MgO (1.06%) and SO_3 (0.12%)	Carbon steel	Plasma spray	The coating was effective to decrease the oxidation and salt corrosion resistance of the carbon steel.
24	1987	Rapp [24]	-	-	-	In-situ electrochemical analysis on hot corrosion, kinetics, morphologies and the mechanisms.
25	2011	Kaushal et al. [25]	Ni-20Cr, 80Ni-Cr	ASTM A213 347H boiler steel	HVOF	The 80Ni-Cr coating was effective in less weight gain and corrosion resistance.
26	2013	Paul et al. [26]	NiCrBSiFe, alloy 718, alloy 625, and alloy C-276	P91	HVOF	The performance of the coatings dependent on its composition and the test conditions. Corrosion stability : alloy 625 > NiCrBSiFe > alloy 718 alloy C-276.
27	2013	Hong et al. [27]	NiCrBSiWFeCoC alloy	AISI 1045 steel	HVOF	The HVOF sprayed NiCrBSiWFeCoC alloy coating - presence of amorphous phase and low porosity and good corrosion resistant.
28	2012	Zhang et al. [28]	CoCrAlSiY coated steel with different Si (0wt%, 2wt%, and 5wt %)	SA-213-T22	HVOF	The increase of Si concentration reduces the average corrosion diffusion depth of the HVOF coating.
29	2017	Shuting et al. [29]	CoCrAlSiY coating with different Si concentrations (0wt%, 2wt% and 5wt%)	GH907	HVOF	Corrosion penetration depth of the coating increases with the rising of temperature, while the increasing of Si concentration decreases the average corrosion penetration depth of the coating
30	2014	Saricimen et al. [30]	Coating, Co_01 Coating, Co_02 Coating, Ni_03	310 stainless steel	HVOF and Plasma spray	Cobalt-based coatings perform better than Nickel-based coating.

31	2007	Sidhu et al. [31]	Cr3C2-NiCr, NiCr, WC-Co and Stellite-6 alloy	ASTM SA213-T11 steel	HVOF	NiCr Coating presented a better corrosive resistance than uncoated steel and WC-Co & Cr_3C_2-NiCr coatings.
32	2020	Shi et al. [32]	Cr_3C_2-NiCr/NiCrAlY	UMCo50 alloy	HVOF	Cr_3C_2-NiCr coating was relatively dense and mainly composed of Cr_3C_2, NiCr, and a minor quantity of Cr_7C_3 three peaks.

To simulate these conditions, we have performed experiments at molten salt (Na_2SO_4–60%V_2O_5) conditions and tested the bare T22 and the above coatings performance. Here the attempt was made to compare the corrosion effect of chromium oxide or silicon dioxide in metal composite HVOF coatings under heat treatment in molten salt conditions. Furthermore, the efforts were made towards the systematic analysis using microscopic, structural and gravimetric changes of bare and HVOF coated at high-temperature molten salt corrosive conditions. Here the oxidative effect of the molten salt mixture at high temperature could aggravate the T22 steel corrosion. Furthermore, investigations were performed to understand the comparative effect of silica and chromium oxides in the HVOF composite coatings. The coated and uncoated samples were exposed to the molten salt environment at 700°C under thermocyclic environments. Corrosion damage was evaluated by using the weight gain method. XRD and SEM/EDS methods to characterize the corroded samples. The high temperature assisted formation of surface metal chromites, chromates and oxide is shown to improve the corrosion stability with chromium oxide coatings. Hence this study is to identify a suitable coating for protecting uncoated T22 steel and to characterize the high-temperature corrosion effect of HVOF-sprayed composite coatings on T22 substrate steel. To develop a reliable laboratory simulation test method for assessing hot corrosion damage, the following methodology is used in this research work, shown in Figure 1.

2. EXPERIMENTAL SECTION

2. 1. Substrate Material T22 steel has been designated as the bare material in the current investigation. For exposure tests, specimens were sectioned from ASTM SA213-T22 steel in square (25 mm × 25 mm × 5 mm) shapes. Sectioned specimens were grit blasted with aluminum oxide before HVOF formulation. The drum jigs were rotated on a turntable during spraying to ensure the application of uniform coatings with a limited edge effect. Table 2 illustrates the nominal chemical composition for T22 substrate steel.

2. 2. Formulation of the Coatings HVOF method was employed to deposit NiCrMoFeCoAl-30%SiO_2 and NiCrMoFeCoAl-30%Cr_2O_3 composite coatings on the T22 substrate steel. The coating powders having particle size in the range of 45 - 60 μm range. The steel tubes utilized in fabrication of boilers face high temperatures [33]. HVOF coating parameters are listed in Table 3. The compositions of the powders utilized in the present examination are tabulated in Table 4. All the standard spray parameters and the spray distance were reserved constant all over the coating procedure. The average coating thickness obtained was 197 μm. The coatings were accumulated on all six edges of the base metal. The grit blasting was executed to get a fine surface roughness and stimulate the best possible adhesion between substrate and coating. SEM coupled with EDAX is used to study the microstructure and the compositions of the specimens. XRD technique was used to analyze the phases of coatings.

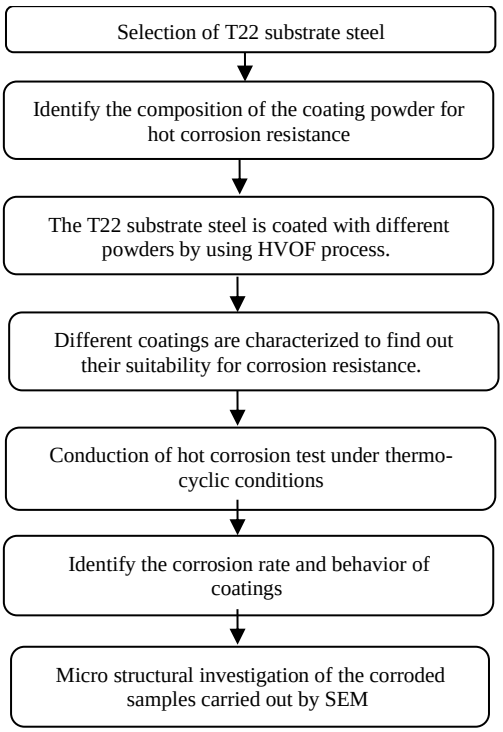

Figure 1. Scheme of coating process and characterization

TABLE 2. Chemical composition (wt%) of T22 substrate steel

Fe	Ni	Cr	Ti	Al	Mo	Mn	Si	C
Bal.	-	2.55	-	-	1.10	0.52	0.43	0.14

TABLE 3. Coating parameters used for HVOF spray process

HVOF process parameter	Quantity units
Oxygen flow rate	250 l/min
Fuel (LPG) flow rate	65-70 l/min
Air-flow rate	550 l/min
Spray distance	178 mm
Powder feed rate	28 g/min
Fuel (LPG) pressure	681 kPa
Oxygen pressure	981 kPa
Air pressure	588 kPa

TABLE 4. Chemical composition of the composite coatings (wt %) used in this study

HVOF coatings	Ni	Cr	Mo	Fe	Co	Al	SiO_2	Cr_2O_3
NiCrMoFeCoAl-30%SiO_2	39.9	15.4	2.1	4.9	4.2	3.5	30	-
NiCrMoFeCoAl-30%Cr_2O_3	39.9	15.4	2.1	4.9	4.2	3.5	-	30

2. 3. Coatings Characterization Techniques An image analyzer (Metaplus software) helps to compute the composite coatings' porosity based on ASTM B276. The mean value of the eight readings was computed for each specimen to evaluate coated steel's porosity. The SEM helped to obtain a cross-sectional micrograph of composite coatings. An inverted metallurgical microscope (OLYMPUS BX53M UPRIGHT METALLURGICAL MICROSCOPE) helps to evaluate the coating thickness. The composite coatings microhardness was evaluated using the Micro Vickers Hardness tester (VH1102, Reva University Bangalore) at a load of 300g at eight different locations on the cross-section a coated specimen. After the surface characterization techniques, the specimens were sectioned, mounted in transoptic powder, and exposed to polishing. The diamond paste (0.3 μm) helped to obtain a mirror finishing. The X-ray diffractometer did an XRD analysis on the coated and uncoated surface. It is operated by using CuKα as radiation at 40 kV and 30 mA. The samples were scanned within the 2θ range of 10° to 80°. SEM/EDAX analysis technique helps to characterize the surface, cross-sectional composition, & morphologies of the coated and uncoated specimens.

2. 4. Cyclic High Temperature Corrosion Test High temperature corrosion studies were performed in a (Na_2SO_4–60%V_2O_5) molten salt solution for 50 cycles under thermocyclic conditions, with each cycle comprised of 1 h of heating in the furnace at 700^0C, followed by 20 min cooling at ambient temperature [34]. The silicon carbide tube furnace is shown in Figure 2. The experimental conditions were selected to replicate the environment in energy-producing units such as furnaces and boilers [35-38]. The silicon carbide tube heater was standardized to the precision of ±5°C utilizing a Pt/Pt–13% Rh thermocouple. Before testing, the physical measurements of the samples were noted carefully with a vernier caliper to measure their dimensions. For comparison, the hot corrosion testing was performed on HVOF coated & bare specimens. The bare and coated specimens were mirror-polished with 1 μm by Al_2O_3 wheel-cloth polishing earlier than the corrosion test. A molten salt of Na_2SO_4–60%V_2O_5 is systematically blended with distilled water. The molten salt was applied uniformly and the coating distribution varies in the range of 3-5 mg/cm^2 on preheated specimens at 250^0C. The salt-coated sample was dehydrated at 100 °C for 3–4 h in the oven. Subsequently, the dehydrated salt-coated sample preserved in the alumina boat was balanced before the high-temperature corrosion test. Each specimen was positioned in the crucible and the weight was evaluated along with the boat and variance in weight data had been remarked. Weight-change data were determined at the end of each cycle. The surfaces of the corroded samples were visually examined to record the color, luster, peeling, and spalling of the scale. After the corrosion studies, the corroded surfaces were investigated by XRD and SEM/EDS techniques.

3. RESULTS

3. 1. Characterization for As-deposited Coatings The coating thickness has been measured from the optical microscope is around 200 μm. The microhardness of HVOF composite coatings is exhibited in Figure 3. Microhardness tests were performed using the model VH1102 auto to determine the microhardness of coated specimens along the cross-section with a load of 300g and a dwell period of 10s. The microhardness of the T22 substrate steel is measured to be around 270 $HV_{0.3}$. The average microhardness values of the NiCrMoFeCoAl-30%SiO_2 and NiCrMoFeCoAl-30%Cr_2O_3 composite

Figure 2. The silicon carbide tube furnace used for high temperature corrosion studies

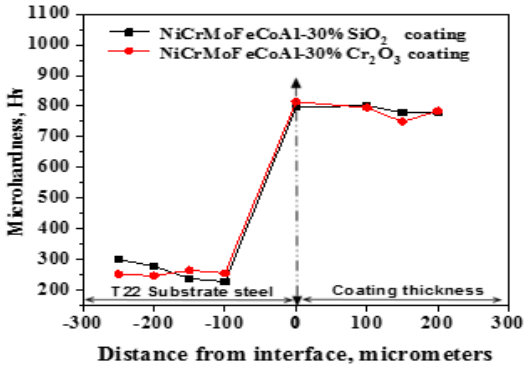

Figure 3. Cross-sectional microhardness profile for HVOF coatings across the cross-section

coatings have been determined to be around 801.9 $HV_{0.3}$ and 814.3 $HV_{0.3}$, respectively. The porosity of these coatings is less than 1.6%. The characterizations of coatings are tabulated in Table 5.

3. 2. Visual Examination Figures 4 (a)-4(c) demonstrates the macrographs of the uncoated T22 steel, NiCrMoFeCoAl-30%SiO_2, and NiCrMoFeCoAl-30%Cr_2O_3 composite coatings are exposed to hot corrosion. The uncoated T22 steel (Figure 4a) appears to dark grey colored oxide scale during the 1st cycle and turned to blackish gray color in the 10th cycle, and the color remains similar up to the end of the cycle. The formation of scales on the T22 substrate steel was determined to be friable and revealed the rupture on a surface. Throughout the early hot corrosion cycles, the formation of the spalling of the oxide scale on the T22 substrate steel was remarked. The NiCrMoFeCoAl-30%SiO_2 coated (Figure 4b) specimen appeared as a faded brown color in the 10th cycle and remains the same until the 50th cycle. The dark gray color of the NiCrMoFeCoAl-30%Cr_2O_3 coated (Figure 4c) specimen changes to grey color in the 10th cycle and remains identical till the end of the corrosion study. Until the end of the high-temperature corrosion study, these composite coatings have not shown any severe spalling of scale, no peeling-off, and no visible cracks on coating layers.

TABLE 5. Variation of porosity, microhardness, and coating thickness of HVOF coated samples

HVOF coatings	Porosity (%)	Vickers Microhardness, VHN (GPa)	Coating thickness (μm)
NiCrMoFeCoAl-30%SiO_2	1.69	801.9 HV 0.3	197
NiCrMoFeCoAl-30%Cr_2O_3	1.66	814.3 HV 0.3	197

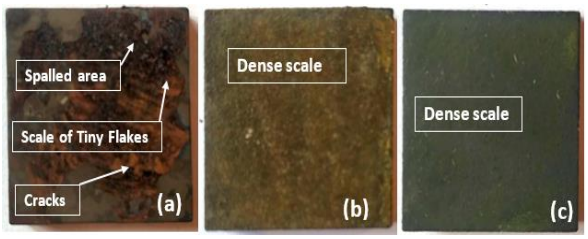

Figure 4. Macro images of the uncoated (a) T22 substrate steel and HVOF coated (b) NiCrMoFeCoAl-30%SiO_2 (c) NiCrMoFeCoAl-30%$Cr2O_3$ specimens are subjected to Na_2SO_4–60%V_2O_5 environment at 700°C

3. 3. Corrosion Kinetics in Molten Salt The weight change per unit area to the no. of cycles is plotted for the T22 steel, NiCrMoFeCoAl-30%SiO_2, and NiCrMoFeCoAl-30%Cr_2O_3 composite coatings are subjected to hot corrosion under thermocyclic conditions are shown in Figure 5(a). The weight gain expeditiously rises up to the 10th cycle in T22 substrate steel. After continuing rise in weight gain is remarked until the 50 cycles. The net weight change of the samples in the molten salt environment signifies the combined effects of the weight loss due to the oxide scales of suspected fluxing and spalling and the weight gain owing to the oxide scale formations. The T22 substrate steel exhibited more differences in the weight change as compared to that of composite coatings. The plot of (weight change/area)^2 vs. no. of cycles for coated and uncoated specimens are presented in Figure 5(b). It can be noted from the graph that T22 steel exhibited some deviations from the parabolic rate law, while composite coatings followed the parabolic rate law. The formation of a thick oxide scale due to the chemical reaction of the composite coatings, T22 substrate steel showed higher weight gain than the NiCrMoFeCoAl-30%SiO_2 and NiCrMoFeCoAl-30%Cr_2O_3 composite coatings. Figure 5(b) clarifies that coated and uncoated specimens in a hot corrosion environment obey the parabolic rate law. *kp* is resulting from the experimental correlation of parabolic rate law Equation (1):

$$(\Delta W/A)^2 = kp \times t \quad (1)$$

where ΔW is the change in weight of T22 steel for initial weight, A signifies per unit area and t signifies the duration for oxidation in sec. The plot of cumulative weight gain is shown in Figure 6. The hot corrosion resistance of coated and uncoated samples, based on cumulative weight gain, remarked as follows:
Uncoated T22 substrate steel ≥ NiCrMoFeCoAl-30%SiO_2 Coated Steel ≥ NiCrMoFeCoAl-30%Cr_2O_3 Coated Steel.

Table 6 illustrates the cumulative weight gain and k_p values of uncoated and coated specimens.

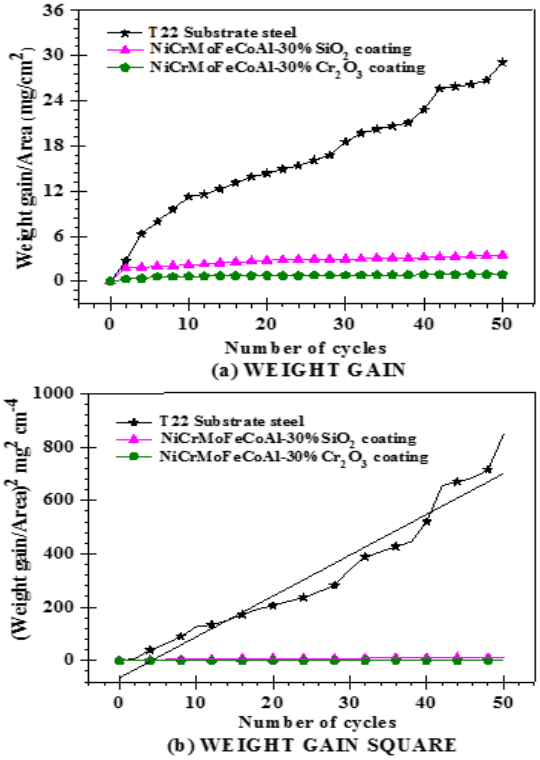

Figure 5. Hot corrosion plots of (weight gain/area) and (weight gain/area)^2 vs. time (h) for bare and composite coated steels subjected to the hot corrosion at 700^{0}C

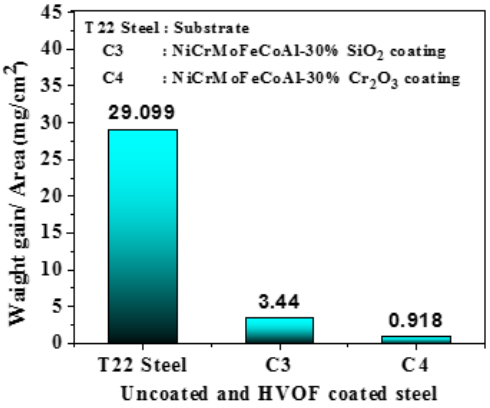

Figure 6. Total weight gain of uncoated T22 steel and composite coated steels subjected to the hot corrosion at 700^{0}C

TABLE 6. Calculated values of the total weight gain and kp

Specimens	Cumulative Weight gain (mg/ cm^2)	k_p g^2/cm^4/s^1
T22 substrate steel	29.099	4.2486×10^{-9}
NiCrMoFeCoAl-30%SiO_2 coating	3.4408	5.2869×10^{-11}
NiCrMoFeCoAl-30%Cr_2O_3 coating	0.9186	3.7972×10^{-11}

3. 4. XRD Analysis of the Oxide Phase Constituents

The XRD profiles for phase ID of the scales composed on corroded T22 substrate steel and composite coatings are depicted in Figures 7(a-c). Fe_2O_3 has been recognized as the major constituent in the scale of the T22 substrate steel along with the minor phases of Cr_2S_3, $NaVO_3$, and NaV_2O_5 on their surface are demonstrated in Figure 7(a). In the case of NiCrMoFeCoAl-30%SiO_2 composite coating is found to have a presence of major phases as SiO_2, Al_2SiO_5, $CoSi_2$, Al_2O_3, and $Cr_2(SO_4)_3$ along with some minor phases of Fe_2SiO_4, $FeVO_4$ & Cr_3Si are compiled in Figure 7(b). In the case of NiCrMoFeCoAl-30%Cr_2O_3 composite coating is found to have a presence of major phases as Cr_2O_3, $NaVO_3$, & $NiCr_2O_4$ together with minor phases of $AlFeO_3$ and Co_3Fe_7 were detected in Figure 7(c). The high temperature assisted formation of metal chromites and chromates could further enhance the corrosion stability.

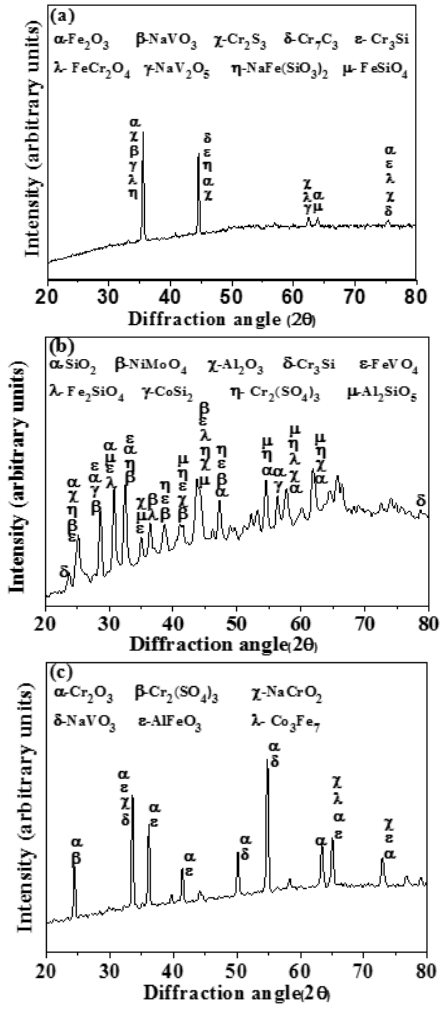

Figure 7. XRD patterns for uncoated (a) T22 substrate steel and HVOF coated (b) NiCrMoFeCoAl-30%SiO_2 (c) NiCrMoFeCoAl-30%Cr_2O_3 specimens exposed to hot corrosion at 700 °C

3. 5. SEM/EDS Analysis of the Oxide Scales The SEM/ EDS micrographs depicting the surface morphology of T22 substrate steel and composite coatings which are subjected to hot corrosion is shown in Figure 8(a-c). The EDS analysis is specified in some selected areas and EDS spots on the surface of the exposed specimens. The formation of oxide scales on the uncoated T22 steel had a rough surface. Black spots, suspected swelling, and scale spallation were observed on the surface. The EDS analysis of T22 substrate steel mainly consists of Fe_2O_3 in a major quantity, and a minor quantity of NiO, V_2O_5, Cr_2O_3, and SiO_2 scales were detected at EDS spot 1. The formation of Fe_2O_3, Al_2O_3, and MnO_x scales are identified at selected area 1 (Figure 8a). The oxide scale of hot corroded T22 boiler tube steel is principally comprised of a hematite (Fe_2O_3) oxide scale as supported by EDS, XRD, and cross-sectional analysis. The formation of the hematite (Fe_2O_3) oxide scale has been analyzed and reported as a non-protective scale, during the failure study of superheater tubes due to fireside corrosion [39, 40]. The SEM/EDS depicting the surface morphology of NiCrMoFeCoAl-30%SiO_2 composite coated specimen demonstrated in Figure 8(b), the formation of SiO_2, Cr_2O_3, and Al_2O_3 at EDS spot 1. Al_2O_3, SiO_2, Mo_2O_3, and Fe_2O_3 scales were observed at selected area 1. The oxide scale on the NiCrMoFeCoAl-30%Cr_2O_3 composite coated specimen (Figure 8c) has a massive structure. The formation of scales mainly consists of Cr_2O_3, V_2O_5. NiO and Na_2O at selected area1. Cr_2O_3, Na_2O, V_2O_5, and Al_2O_3 scales were detected at EDS spot 1. The overall surface scale formed on coated specimens to be dense clusters, continuous and uniform structure and there is no spallation and crack free. The formation of Cr_2O_3, Na_2O, SiO_2, and Al_2O_3 presence of noted phases are observed in both XRD and EDS analysis and it has been proved.

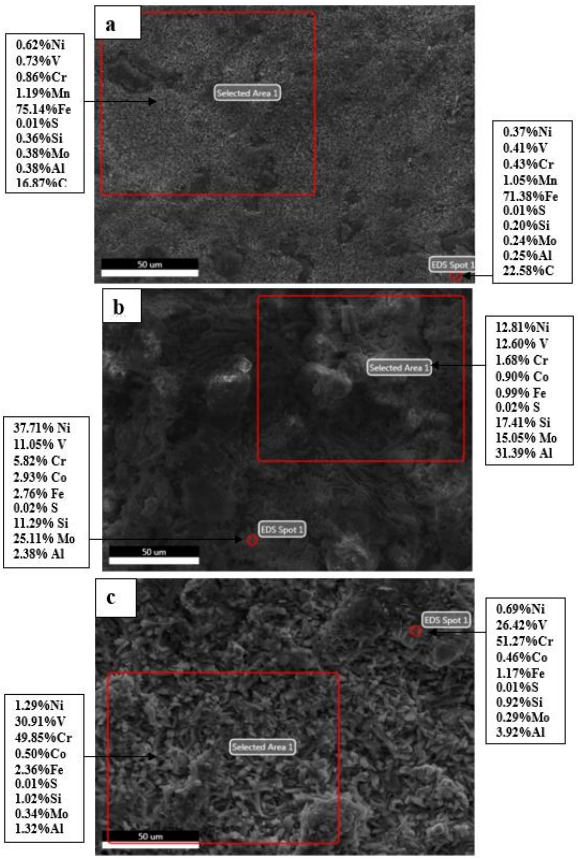

Figure 8. SEM / EDS surface analysis for the bare and coated specimens after hot corrosion test at 700°C

3. 6. Cross-sectional SEM/EDS Analysis of the Oxide Scales SEM/EDS and BSEI cross-sectional investigation of hot corroded specimens are presented in Figures 9(a) and 9(b). EDS has been taken at different points throughout the scale, coating, and substrate. The oxide scale formed was non-porous and dense in the composite coatings. The formation of oxide scales on the cross-section of NiCrMoFeCoAl-30%SiO_2 coated steel can be remarked from Figure 9(a). The scale's top layer (point 1) comprises Fe, C, Cr, & Ni with oxygen. Point 2 indicates the presence of Ni, Cr, Mo, & Co oxide scales. Further, in point 3, the interface between substrate and coating consists of Ni, Cr, Co, and Mo oxide scales are identified. Elemental variation through the cross-section of NiCrMoFeCoAl-30%Cr_2O_3 coated steel exhibited in Figure 9(b), the presence of Cr, O, & V are in a rich amount, along with the fair amount of Ni and a lower amount of Al, Mo, Na, and Co oxide scales are identified at point 1. Point 2, specifies the presence of Ni, Cr, and Co oxides scales. Point 3 depicts the existence of Fe, Al, & Cr, together with oxygen at the interface between the coating and substrate. A crack-free, continuous, lamellar, dense, and uniform oxide scales are formed on the coated specimen.

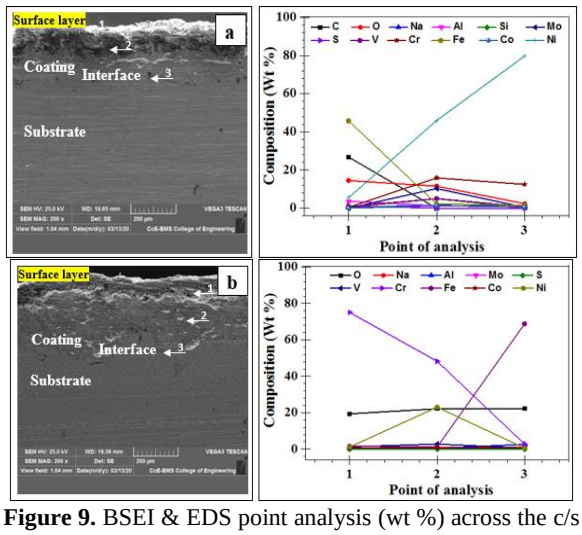

Figure 9. BSEI & EDS point analysis (wt %) across the c/s of the composite coated (a) NiCrMoFeCoAl-30%SiO_2 (b) NiCrMoFeCoAl-30%Cr_2O_3 samples after hot corrosion test

4. DISCUSSIONS

The cumulative observations of the above microscopic, structural and gravimetric analysis evident the progressive corrosion of uncoated T22 steel and the severe corrosion under molten salt conditions. The porous nature of the hot corroded products could further allow the propagation of corrosion. The high weight gain was observed with uncoated T22 while the lowest was with 30% Cr_2O_3 containing coatings. The high-temperature effects along with Na_2SO_4-60%V_2O_5 further enhance the oxidative process of the uncoated T22. However, both the HVOF coatings show improved stability in term of weight gain kinetic analysis. The significance of gravimetric data analysis is to determine the augmented kinetics induced by the Na_2SO_4-60%V_2O_5 eutectic mixture. The thick oxide scale formed on bare T22 steel predominantly comprises of iron oxide on hot corroded T22 steel, suggest the higher hot corrosion rate. This is further enhanced by the existence of other metal oxides which is observed in SEM/EDS and XRD analysis. As the consequence of the presence of higher valent metal ions, there could be an increase in the local acidic nature along with molten salt mixture on the T22 surface. This could result in the acidic fluxing of the protective oxides and impart more porous oxide scale which progressively allows the aggressive gaseous mixture to reach the base metal surface at high temperature. The hot corrosion kinetics of the NiCrMoFeCoAl-30%SiO_2 coated steel showed parabolic behavior. The oxides of SiO_2, Mo_2O_3, and V_2O_5 formed on the surface have minimal solubility in the highly acidic and oxidative salt environment. Also coefficient of thermal expansion of these oxides are in close range and hence the thermal stresses are minimized. The oxide scales formed on the coated steel are adherent and dense without any scale spalling and cracking. The oxide scales formed effectively protect the substrate alloy, as the cyclic oxidation behavior of all the coatings is dictated mainly by the scale spallation resistance. The superior hot corrosion resistance of NiCrMoFeCoAl-30%Cr_2O_3 can be attributed to the thick protective oxide scale developed on the surface. The uppermost layer of the oxide scale mainly contains oxides and spinel oxides of Cr and Ni and O which have minimal solubility in highly acidic Na_2SO_4-60%V_2O_5 melt. These oxides act as a barrier to the diffusion of O_2 and corrosive species of molten salt into the inside of the coating, hence the coating region beneath this oxide scale remains unoxidized. Slow oxidation kinetics and parabolic behavior observed during the gravimetric studies show a diffusion-limited reaction rate. During the initial stages of hot corrosion, the formation of Cr_2O_3 from the chromium oxide prevents the preferential oxidation of Ni and Cr. The refractory Ni and Cr are a strengthener to maintain the mechanical properties of the coating. The hot corroded HVOF coating containing Cr_2O_3 forms metal chromites, chromates and oxides which could further enhance the protection against the progressive corrosion. Also, the cross-sectional view of the heat-treated Cr_2O_3 containing coating shows less porous and high dense compared to SiO_2. This protects the base T22 from the access of corroding species at high temperature. This further supports the enhanced corrosion resistance of NiCrMoFeCoAl-30%Cr_2O_3 than the SiO_2 based composite coating.

5. CONCLUSIONS

In the current investigation, the composite coatings were deposited on uncoated T22 steel and the behavior of high-temperature corrosion was studied. From the analysis, the following conclusions are drawn:

1. The NiCrMoFeCoAl-30%SiO_2 and NiCrMoFeCoAl-30%Cr_2O_3 composite coatings are effectively deposited by the HVOF process on T22 substrate steel. The coating thickness was around 200 μm.
2. The uncoated T22 steel has suffered peeling of scale, intense spelling, and tremendous weight gain. The weight gain of the NiCrMoFeCoAl-30%SiO_2 and NiCrMoFeCoAl-30%Cr_2O_3 coated specimens were 88.17% and 96.84% respectively, lower than that of the uncoated T22 steel in the molten salt environment at 700^0C under thermocyclic conditions
3. NiCrMoFeCoAl-30%Cr_2O_3 coated T22 steel shows the existence of Cr_2O_3 was encountered as a principal phase and NiCrMoFeCoAl-30%SiO_2 coated T22 steel shows the presence of Al_2O_3 and SiO_2 were encountered as principal phases in the molten salt environment at 700^0C by SEM/EDS and XRD analysis.
4. The corrosion resistance of composite coatings are improved as compared to the substrate specimen. The corrosion resistance of coated and uncoated specimens presented in the following order:

NiCrMoFeCoAl-30%Cr_2O_3 coating> NiCrMoFeCoAl-30%SiO_2 coating> T22 substrate steel. The HVOF composite coating containing chromium oxides shows enhanced high-temperature heating stability compared to silica composite.

6. ACKNOWLEDGMENT

Authors thanks REVA University and BMSCE for surface and structural characterization facilities.

7. REFERENCES

1. Ebrahimi, N., Sedaghat Ahangari Hosseinzadeh, A., Vaezi, M. and Mozafari, M., "Evaluation of corrosion resistance of bi-

layered plasma-sprayed coating on titanium implants", ***International Journal of Engineering*, *Transactions A: Basics,*** Vol. 35, No. 4, (2022), 635-643, doi: 10.5829/ije.2022.35.04A.03.

2. Veda Spandana, V., Jamuna Rani, G., Venkateswarlu, K. and Venu Madhav, V., "Experimental study on yttria stabilized and titanium oxide thermal barrier coated piston effect on engine performance and emission characteristics", ***International Journal of Engineering*, *Transactions C: Basics,*** Vol. 34, No. 12, (2021), 2611-2616, doi: 10.5829/ije.2021.34.12c.05.
3. Rahnavard, M., "Hot corrosion behavior of functional graded material thermal barrier coating (research note)", ***International Journal of Engineering*, *Transactions A: Basics,*** Vol. 30, No. 1, (2017), 101-108, doi: 10.5829/idosi.ije.2017.30.01a.13.
4. Mahdipoor, M.S. and Rahimipour, M.R., "Comparative study of plasma sprayed yittria and ceria stabilized zirconia properties", ***International Journal of Engineering*, *Transactions A: Basics,*** Vol. 26, No. 1, (2013), 13-18, doi: 10.5829/idosi.ije.2013.26.01a.02.
5. NAEIMI, F. and Tahari, M., "Effect of surface morphologies on the isothermal oxidation behavior of mcraly coatings fabricated by high-velocity oxyfuel processes", ***International Journal of Engineering*, *Transactions C: Basics,*** Vol. 30, No. 3, (2017), 432-438, doi: 10.5829/idosi.ije.2017.30.03c.13.
6. Singh, S., Goyal, K. and Goyal, R., "Performance of cr3c2-25 (ni-20cr) and ni-20cr coatings on t91 boiler tube steel in simulated boiler environment at 900° c", ***Chemical and Materials Engineering***, Vol. 4, No. 4, (2016), 57-64, doi: 10.13189/cme.2016.040401.
7. Ak, N., Tekmen, C., Ozdemir, I., Soykan, H. and Celik, E., "Nicr coatings on stainless steel by hvof technique", ***Surface and Coatings Technology***, Vol. 174, (2003), 1070-1073, doi: 10.1016/S0257-8972(03)00367-0.
8. Sidhu, H.S., Sidhu, B.S. and Prakash, S., "Evaluation of the hot corrosion behavior of lpg assisted hvof nicr wire sprayed boiler tube steels in molten salt environments", ***ISIJ International***, Vol. 46, No. 7, (2006), 1067-1074, doi: 10.2355/isijinternational.46.1067.
9. Uusitalo, M., Vuoristo, P. and Mäntylä, T., "High temperature corrosion of coatings and boiler steels in oxidizing chlorine-containing atmosphere", ***Materials Science and Engineering: A***, Vol. 346, No. 1-2, (2003), 168-177, doi: 10.1016/S0921-5093(02)00537-3.
10. Wang, B., Geng, G. and Levy, A., "Erosion and erosion-corrosion behavior of chromized-siliconized steel", ***Surface and Coatings Technology***, Vol. 54, (1992), 529-535, doi: 10.1016/S0257-8972(07)80077-6.
11. Rapp, R.A., "Hot corrosion of materials: A fluxing mechanism?", ***Corrosion science***, Vol. 44, No. 2, (2002), 209-221, doi: 10.1016/S0010-938X(01)00057-9.
12. Goyal, K., Singh, H. and Bhatia, R., "Hot-corrosion behavior of cr2o3-cnt-coated astm-sa213-t22 steel in a molten salt environment at 700° c", ***International Journal of Minerals, Metallurgy, and Materials***, Vol. 26, No. 3, (2019), 337-344, doi: 10.1007/s12613-019-1742-8.
13. Mahesh, R., Jayaganthan, R. and Prakash, S., "Evaluation of hot corrosion behaviour of hvof sprayed ni–5al and nicral coatings in coal fired boiler environment", ***Surface engineering***, Vol. 26, No. 6, (2010), 413-421, doi: 10.1179/174329409X451164.
14. Wang, C.-J. and Lin, J.-S., "The oxidation of mar m247 superalloy with na2so4 coating", ***Materials Chemistry and Physics***, Vol. 76, No. 2, (2002), 123-129, doi: 10.1016/S0254-0584(01)00527-2.
15. Sidhu, V.P.S., Goyal, K. and Goyal, R., "Hot corrosion behaviour of hvof-sprayed 93 (wc-cr3c2)-7ni and 83wc-17co coatings on boiler tube steel in coal fired boiler", ***Australian Journal of Mechanical Engineering***, Vol. 17, No. 2, (2019), 127-132, doi: 10.1080/14484846.2017.1364834.
16. Sreenivasulu, V. and Manikandan, M., "Hot corrosion studies of hvof sprayed carbide and metallic powder coatings on alloy 80a at 900° c", ***Materials Research Express***, Vol. 6, No. 3, (2018), 036519, doi: 10.1088/2053-1591/aaf65d.
17. Chatha, S.S., Sidhu, H.S. and Sidhu, B.S., "High temperature hot corrosion behaviour of nicr and Cr_3C_2–nicr coatings on t91 boiler steel in an aggressive environment at 750 c", ***Surface and Coatings Technology***, Vol. 206, No. 19-20, (2012), 3839-3850, doi: 10.1016/j.surfcoat.2012.01.060.
18. Loghman-Estarki, M., Razavi, R.S., Edris, H., Bakhshi, S., Nejati, M. and Jamali, H., "Comparison of hot corrosion behavior of nanostructured scysz and ysz thermal barrier coatings", ***Ceramics International***, Vol. 42, No. 6, (2016), 7432-7439, doi: 10.1016/j.ceramint.2016.01.147.
19. Aadhavan, R., Bhanuchandar, S. and Babu, K.S., "Surface coating of ceria nanostructures for high-temperature oxidation protection", ***Materials Research Express***, Vol. 5, No. 4, (2018), 045025, doi: 10.1088/2053-1591/aaba46.
20. Somasundaram, B., Kadoli, R. and Ramesh, M., "Hot corrosion behaviour of hvof sprayed (Cr_3C_2–35% nicr)+ 5% si coatings in the presence of na2so4–60% v2o5 at 700° c", ***Transactions of the Indian Institute of Metals***, Vol. 68, No. 2, (2015), 257-268, doi: 10.1007/s12666-014-0453-0.
21. Mangla, A., Chawla, V. and Singh, G., "Comparative study of hot corrosion behavior of hvof and plasma sprayed Ni20Cr coating on sa213 (t22) boiler steel in Na_2SO_4-60% v2o5 environment", ***International Journal of Engineering Sciences & Research Technology***, Vol. 4, No. 11, (2017), 2348-8034, doi: 10.5281/zenodo.1037655.
22. Kaur, M., Singh, H. and Prakash, S., "High-temperature behavior of a high-velocity oxy-fuel sprayed Cr_3C_2-nicr coating", ***Metallurgical and Materials Transactions A***, Vol. 43, No. 8, (2012), 2979-2993, doi: 10.1007/s11661-012-1118-4.
23. Sidhu, B.S., Singh, H., Puri, D. and Prakash, S., "Wear and oxidation behaviour of shrouded plasma sprayed fly ash coatings", ***Tribology International***, Vol. 40, No. 5, (2007), 800-808, doi: 10.1016/j.triboint.2006.07.006.
24. Rapp, R.A., "Chemistry and electrochemistry of hot corrosion of metals", ***Materials Science and Engineering***, Vol. 87, (1987), 319-327, doi: 10.1016/0025-5416(87)90394-6.
25. Kaushal, G., Singh, H. and Prakash, S., "High temperature corrosion behaviour of hvof-sprayed Ni-20Cr coating on boiler steel in molten salt environment at 900° c", ***International Journal of Surface Science and Engineering***, Vol. 5, No. 5-6, (2011), 415-433, doi: 10.1504/IJSURFSE.2011.044388.
26. Paul, S. and Harvey, M., "Corrosion testing of ni alloy hvof coatings in high temperature environments for biomass applications", ***Journal of Thermal Spray Technology***, Vol. 22, No. 2, (2013), 316-327, doi: 10.1007/s11666-012-9820-8.
27. Hong, S., Wu, Y., Li, G., Wang, B., Gao, W. and Ying, G., "Microstructural characteristics of high-velocity oxygen-fuel (hvof) sprayed nickel-based alloy coating", ***Journal of Alloys and Compounds***, Vol. 581, (2013), 398-403, doi: 10.1016/j.jallcom.2013.07.109.
28. Bala, N., Singh, H., Prakash, S. and Karthikeyan, J., "Investigations on the behavior of hvof and cold sprayed ni-20cr coating on t22 boiler steel in actual boiler environment", ***Journal of Thermal Spray Technology***, Vol. 21, No. 1, (2012), 144-158, doi: 10.1007/s11666-011-9698-x.
29. Shuting, Z., Kaiping, D., Xianjing, R. and Ji, S., "Effect of si on hot corrosion resistance of cocraly coating", ***Rare Metal Materials and Engineering***, Vol. 46, No. 10, (2017), 2807-2811, doi: 10.1016/S1875-5372 (18)30011-0.

30. Saricimen, H., Quddus, A. and Ul-Hamid, A., "Hot corrosion behavior of plasma and hvof sprayed co-and ni-based coatings at 900 c", ***Protection of Metals and Physical Chemistry of Surfaces***, Vol. 50, No. 3, (2014), 391-399, doi: 10.1134/S2070205114030162.

31. Sidhu, H., Sidhu, B. and Prakash, S., "Hot corrosion behavior of hvof sprayed coatings on astm sa213-t11 steel", ***Journal of Thermal Spray Technology***, Vol. 16, No. 3, (2007), 349-354, doi: 10.1007/s11666-007-9029-4.

32. Shi, M., Xue, Z., Liang, H., Yan, Z., Liu, X. and Zhang, S., "High velocity oxygen fuel sprayed cr3c2-nicr coatings against na2so4 hot corrosion at different temperatures", ***Ceramics International***, Vol. 46, No. 15, (2020), 23629-23635, doi: 10.1016/j.ceramint.2020.06.135.

33. Sidhu, B.S. and Prakash, S., "Evaluation of the corrosion behaviour of plasma-sprayed ni3al coatings on steel in oxidation and molten salt environments at 900 c", ***Surface and Coatings Technology***, Vol. 166, No. 1, (2003), 89-100, doi: 10.1016/S0257-8972(02)00772-7.

34. Rani, A., Bala, N. and Gupta, C., "Characterization and hot corrosion behavior of d-gun sprayed Cr_3C_2-75% Al_2O_3 coated astm-sa210-a1 boiler steel in molten salt environment", ***Anti-Corrosion Methods and Materials***, (2017), doi: 10.1108/ACMM-09-2016-1712.

35. Deb, D., Iyer, S.R. and Radhakrishnan, V., "A comparative study of oxidation and hot corrosion of a cast nickel base superalloy in different corrosive environments", ***Materials Letters***, Vol. 29, No. 1-3, (1996), 19-23, doi: 10.1016/S0167-577X (96)00109-7.

36. Wang, C.-J., Chang, Y.-C. and Su, Y.-H., "The hot corrosion of fe-mn-al–c alloy with NaCl/Na_2SO_4 coating mixtures at 750° c", ***Oxidation of Metals***, Vol. 59, No. 1, (2003), 115-133, doi: 10.1023/A: 1023022100300.

37. Zheng, L., Maicang, Z. and Jianxin, D., "Hot corrosion behavior of powder metallurgy rene95 nickel-based superalloy in molten nacl– Na_2SO_4 salts", ***Materials & Design***, Vol. 32, No. 4, (2011), 1981-1989, doi: 10.1016/j.matdes.2010.11.067.

38. Tsaur, C.-C., Rock, J.C., Wang, C.-J. and Su, Y.-H., "The hot corrosion of 310 stainless steel with pre-coated NaCl/ Na_2SO_4 mixtures at 750 c", ***Materials Chemistry and Physics***, Vol. 89, No. 2-3, (2005), 445-453, doi: 10.1016/j.matchemphys.2004.10.002.

39. Bala, N., Singh, H. and Prakash, S., "Accelerated hot corrosion studies of cold spray ni–50cr coating on boiler steels", ***Materials & Design***, Vol. 31, No. 1, (2010), 244-253, doi: 10.1016/j.matdes.2009.06.033.

40. Sidhu, T., Prakash, S. and Agrawal, R., "Characterisations of hvof sprayed nicrbsi coatings on Ni-and Fe-based superalloys and evaluation of cyclic oxidation behaviour of some ni-based superalloys in molten salt environment", ***Thin Solid Films***, Vol. 515, No. 1, (2006), 95-105, doi: 10.1016/j.tsf.2005.12.041.

Persian Abstract

چکیده

پوشش‌های پاشیده شده با سوخت اکسی با سرعت بالا (HVOF) می‌توانند مقاومت در برابر خوردگی فولاد لخت دیگ بخار ASTM SA213-T22 را بهبود بخشند. در این گزارش، ما پوشش‌های کامپوزیت NiCrMoFeCoAl-30% SiO2 و NiCrMoFeCoAl-30% Cr2O3 را بررسی کرده‌ایم که برای محافظت در برابر خوردگی روی فولاد بویلر لخت ASTM SA213-T22 قرار گرفته‌اند. مطالعات خوردگی در دمای بالا در محیط نمک مذاب (Na2SO4-60% V2O5)در دمای ۷۰۰ درجه سانتیگراد تحت شرایط ترمو سیکلیک انجام شد. پوشش های کامپوزیت اسپری شده برای ریزساختار و خواص مکانیکی مشخص می شوند. روش گرما وزنی برای درک سینتیک خوردگی استفاده شد. ویژگی‌های محصولات خوردگی با استفاده از تکنیک‌های میکروسکوپ الکترونی روبشی (SEM)طیف‌سنجی پراکنده انرژی (EDS)و پراش اشعه ایکس (XRD)مورد بررسی قرار گرفت. نتایج به‌دست‌آمده نشان می‌دهد که هر دو پوشش کامپوزیت نسبت به فولاد بویلر لخت ASTM SA213-T22 نسبت به مقاومت در برابر خوردگی مطلوب هستند. پوشش کامپوزیت NiCrMoFeCoAl-30% Cr2O3 به دلیل توزیع یکنواخت ماتریس پوشش کامپوزیت و توسعه حفاظت محافظ Cr2O3 در مقیاس، به این نتیجه رسید که مقاومت در برابر خوردگی برتر را در محیط خوردگی با دمای بالا ارائه دهد. نمک مذاب دارای پوشش حاوی اکسید کروم عملیات حرارتی شده، پایداری خوردگی خوبی نسبت به کامپوزیت سیلیس نشان می دهد. این را می توان به کرومات های فلزی، کرومیت ها و لایه های اکسید به کمک دمای بالا نسبت داد.